Second International Workshop on Seismic Design of Bridges
Queenstown, New Zealand, 9-13 August 1994

DISPLACEMENT BASED SEISMIC DESIGN OF MULTI-DEGREE-OF-FREEDOM BRIDGE STRUCTURES

G.M. Calvi [1] and G.R. Kingsley [2]

1 Dipartimento di Meccanica Strutturale, Università degli Studi di Pavia, Italia
2 Atkinson-Noland and Associates, Boulder Colorado, USA.

ABSTRACT

The concept of displacement-based design is attractive for seismic design, primarily because it places the focus of design directly on displacement demand, and hence damage, rather than on force-reduction or behavior factors. A procedure is presented which extends the simple concept of displacement-based design to complex multi-degree-of-freedom (MDOF) bridge structures. The procedure, analogous in some respects to an equivalent static lateral load procedure, is based on the assumption of a displaced shape for the structure, and the subsequent reduction of the system to an equivalent single-degree-of-freedom (SDOF) system. With the determination of a desired displacement and damping in the equivalent SDOF structure, displacement response spectra are used to determine the required stiffness necessary to achieve the design displacements. The process was shown to work well for the design of a symmetrical bridge, but suffered the same shortcomings of an equivalent force based procedure when applied to a highly irregular bridge with several prominent modes of vibration rather than a single, dominant displaced shape. The topic of design-oriented displacement response spectra is also briefly addressed.

1. INTRODUCTION

There has been growing interest recently in the development of displacement based seismic design procedures for RC structures [4,6]. This has stemmed partly from the recognition that, under seismic actions, displacements provide a more fundamental expression of structural response than forces, and that the structural design process should be oriented accordingly. Since structural damage can be considered to be directly related to displacement demands, it can be controlled most efficiently through the imposition of displacement (or drift) limits rather than strength limits. In the force/strength-based design procedure, however, displacement limits are checked near the end of the design process for serviceability limits, or are considered in terms of ductility demands which are treated indirectly through the use of "behavior factors" or "response coefficients" that modify design forces. Placing design priority on the displacements first, with checks on strength at the end, allows for a much more consistent consideration of damage. Furthermore, displacement-based design offers the ability to explicitly control the displacement demand in each member rather than assigning a single, force-based behavior factor to the entire structure.

The fundamental conceptual shift required in switching from a force-based to a displacement-based design approach was discussed by Priestley [6] for the case of a single degree-of-

freedom (SDOF) bridge pier structure. In a traditional force-based design, the period of vibration of a structure is estimated (or calculated based on previous trial design), and a design acceleration response spectra is entered to determine, for a given level of damping, what the elastic force demand on the structure will be. Alternatively, the required displacement capacity for the structure can be specified, and the displacement response spectra consulted to determine the required period of vibration (stiffness) necessary to achieve it. For simple SDOF structures, the process outlined by Priestley is conceptually clear. Unfortunately, application of the method to more complex MDOF structural systems is not necessarily straight forward, and requires some additional steps. In this paper, a method is proposed to extend the concepts of displacement-based design to the special case of MDOF bridge structures.

The first consideration, applicable to both SDOF and MDOF structures, is the establishment of appropriate design spectra for displacements. While there has been significant effort to develop acceleration response spectra for design, there has been relatively little consideration of the use of displacement spectra. This issue will be discussed briefly below. The second requirement is the development of an equivalent SDOF representation of an MDOF structure such that SDOF design spectra can be used. This will be achieved by imposing a predefined displaced shape on the structure, and establishing the other properties of the equivalent SDOF structure accordingly. Determination of an appropriate displaced shape is certainly one of the most important steps in the process. Following the development of these preliminary steps, the displacement-based design process will be outlined, and example seismic designs of two bridges will be presented, with comparisons to the designs using traditional strength and ductility criteria.

2. RESPONSE SPECTRA

Smoothed elastic response spectra recommended in a recent draft of Eurocode 8 [2] are shown in Figure 1 for a maximum ground acceleration of 0.35g on subsoil class B (as defined in the code). The four regions of the spectra are defined by the following equations

$$0 < T < T_B \qquad S_e(T) = a_g S\left(1 + \frac{T}{T_B}(\eta\beta_o - 1)\right) \tag{1}$$

$$T_B \le T \le T_C \qquad S_e(T) = a_g \eta S \beta_o \tag{2}$$

$$T_C < T \le T_D \qquad S_e(T) = a_g \eta S \beta_o \left(\frac{T_C}{T}\right)^{k1} \tag{3}$$

$$T_D < T \qquad S_e(T) = a_g \eta S \beta_o \left(\frac{T_C}{T_D}\right)^{k1} \left(\frac{T_D}{T}\right)^{k2} \tag{4}$$

where

T	is the vibration period of a linear SDOF system
a_g	is the design ground acceleration (=0.35 g)
β_0	is the maximum normalised spectral value assumed constant between Tb and Tc (=2.5)

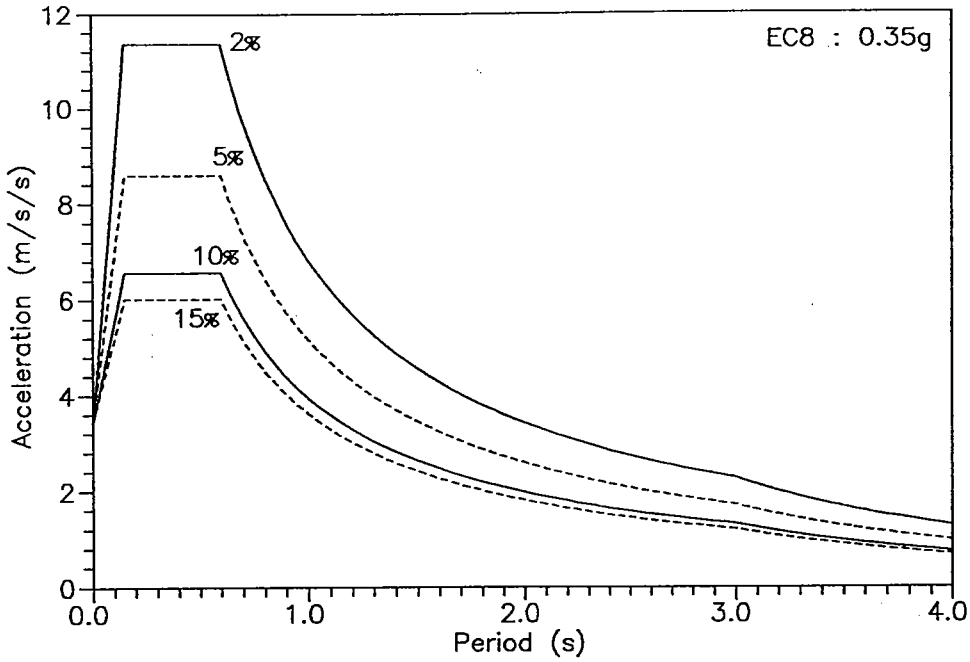

Figure 1 Eurocode 8 Elastic Acceleration Response Spectra for Maximum Ground Acceleration of 0.35 g on Subsoil Class B.

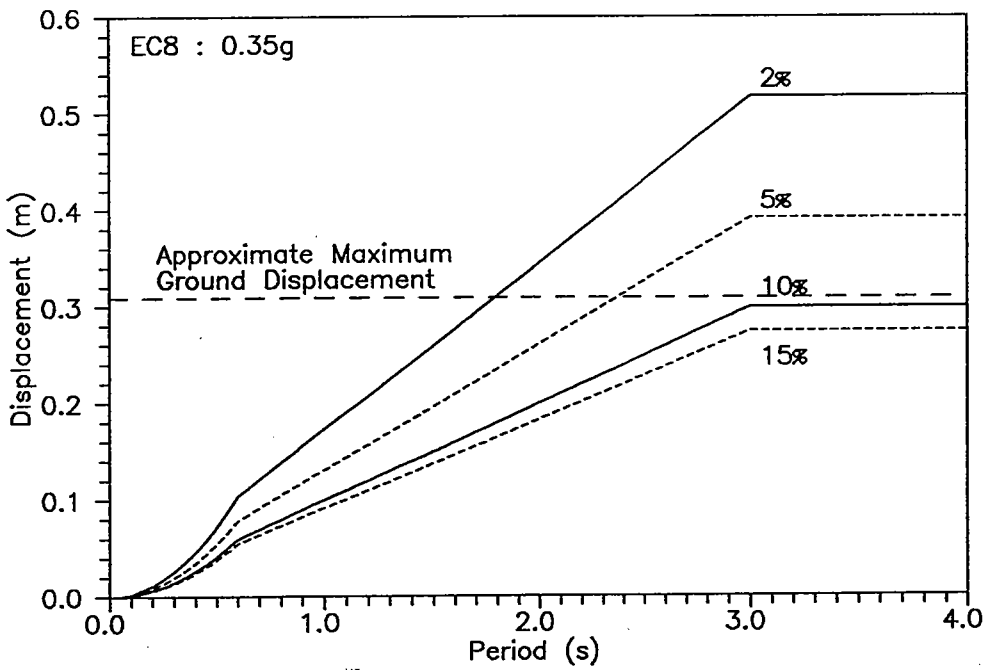

Figure 2 Eurocode 8 Elastic Displacement Response Spectra for Maximum Ground Acceleration of 0.35 g on Subsoil Class B.

T_b,T_c are the limits to the constant spectral acceleration branch (=0.15 and 0.60 respectively)

Td is the value defining the beginning of the constant displacement range of the spectrum (=3.0)

k_1,k_2 are exponents (=1 and 2 respectively)

S is a soil parameter (=1)

η is the damping correction factor given by

$$\eta = \sqrt{\frac{0.07}{0.02+\xi}} \geq 0.7$$

The corresponding displacement spectra, related to the spectral accelerations by a factor of $1/\omega^2$, are shown in Figure 2. Notice that equation (4) for the region $T>T_D$ has a very small influence on the acceleration response, but results in a plateau in the displacement response spectra rather than linearly increasing displacement with increasing period. While the constant displacement zone represents an improvement over simpler design spectra, it creates a problem for displacement-based design, since the period becomes indeterminate for displacements greater than or equal to the plateau value. This may be significant for bridges which could enter the range of very long period structures. In actual displacement spectra, the displacements eventually decrease, with values for all damping levels converging towards the maximum ground displacement. An improved design displacement response spectra could be attained simply by replacing the constant displacement region with displacements decreasing to a single ground displacement at a large period. For example, EC8 [2] recommends, in the absence of more accurate determination, an approximate value for the maximum ground displacement:

$$\delta_g = 0.05 a_g S T_C T_D \qquad (5)$$

This displacement is shown in Figure 2. Since the forces and displacements of large period structures are relatively insensitive to small changes in period, such a simple approximation would probably be sufficient.

It is convenient, for either displacement-based or force-based design, to plot design spectra in terms of both accelerations and displacements, as shown in Figure 3. Lines of constant period becomes a series of radial lines in this representation. With such a plot, the designer can maintain the primary focus on displacements without losing sight of the consequences of design decisions on the forces. Examples of spectra generated from earthquake records from the 1971 San Fernando earthquake and the 1979 Imperial Valley earthquake are plotted in terms of acceleration and displacements in Figure 4. With this representation, it is evident, for example, that a change in period from 1.5 to 2.0 seconds results in a significant drop in accelerations with nearly constant maximum displacement for the Imperial Valley College record; conversely, the same change in period for the Anderson road record results in a dramatic increase in displacements with nearly constant maximum acceleration.

3. DEFINITION OF THE EQUIVALENT SDOF STRUCTURE

With the assumption of a displaced shape, an MDOF structure may be completely described in terms of a single degree of freedom. Consider an n DOF structure, such as the one represented in Figure 5 by a simplified model of a three-pier bridge. It is desired to define an equivalent SDOF structure with mass m_e, stiffness K_e, damping ξ_e and with effective

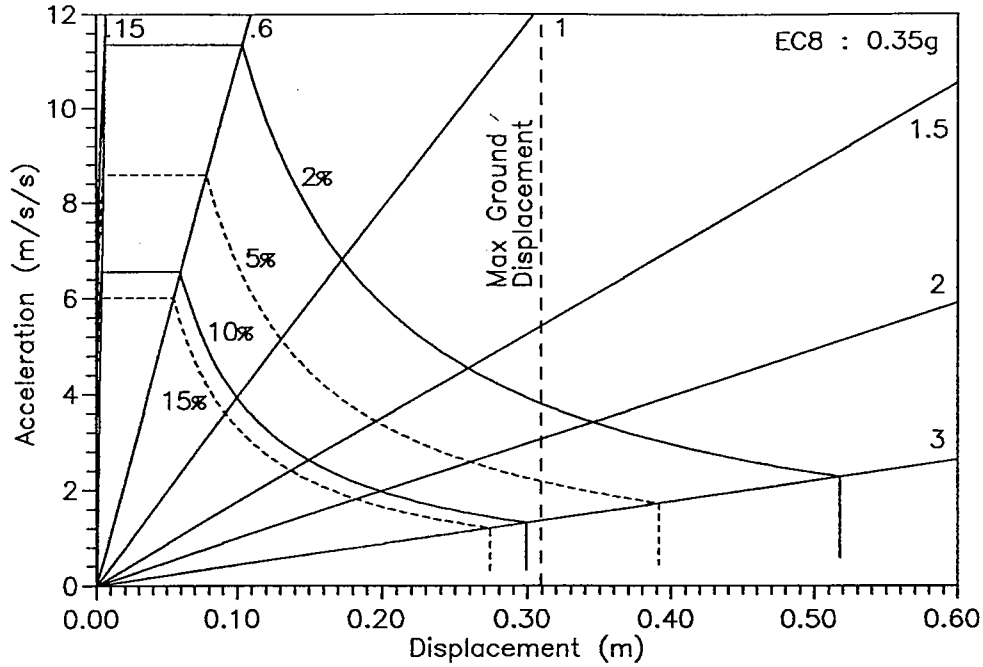

Figure 3 Combined Acceleration and Displacement Response Spectra for Design

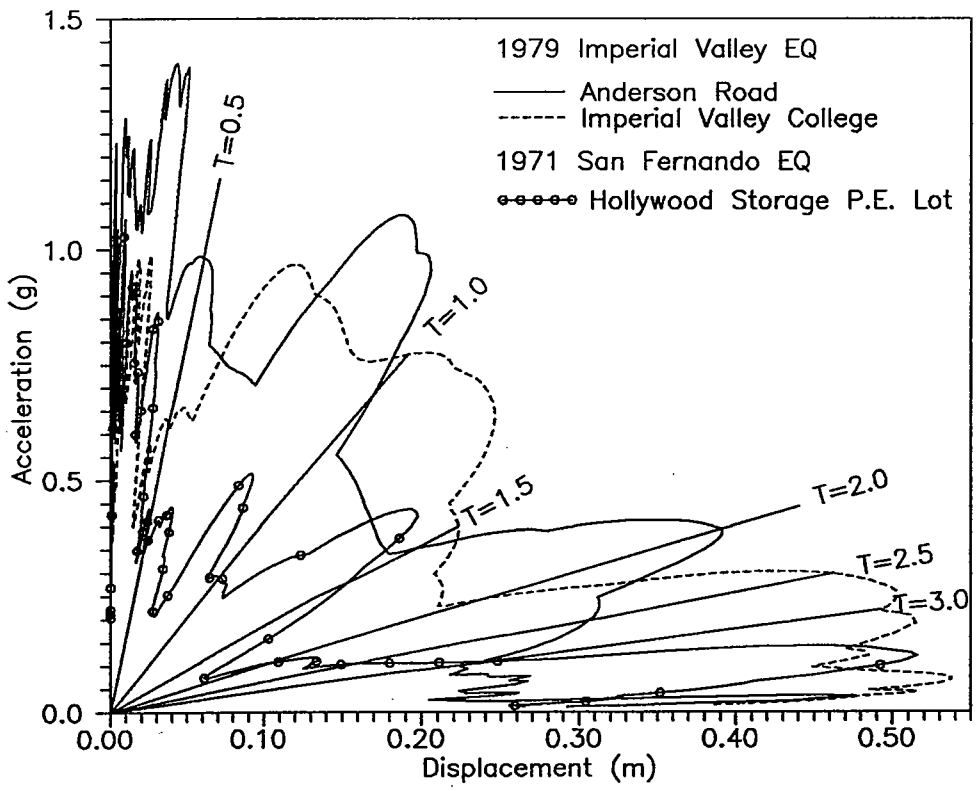

Figure 4 Combined Acceleration and Displacement Response Spectra from the 1979 Imperial Valley and 1971 San Fernando earthquakes.

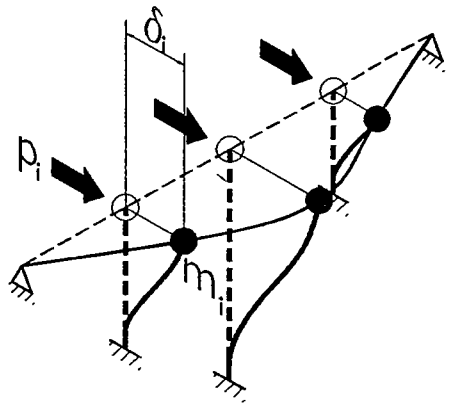

Figure 5 Idealised MDOF Bridge Structure

displacements and forces equal to δ_e and p_e respectively. We first define a constant displaced shape in terms of n factors c_i such that

$$\delta_i = c_i \delta_e \tag{6}$$

We also assume that the acceleration at each DOF is proportional to the same displaced shape, thus

$$a_i = c_i a_e \tag{7}$$

We require that the total applied force be equal for the MDOF and SDOF systems, thus

$$p_e = \sum_{i=1}^{n} p_i = \sum_{i=1}^{n} m_i a_i = a_e \sum_{i=1}^{n} m_i c_i \tag{8}$$

The effective mass of the equivalent SDOF structure can therefore be expressed as

$$m_e = \sum_{i=1}^{n} m_i c_i \tag{9}$$

The inertial forces at the individual DOF can be expressed in terms of the equivalent SDOF force

$$p_i = m_i a_i = m_i c_i a_e = p_e \frac{m_i c_i}{\sum_{k=1}^{n} m_k c_k} \tag{10}$$

Substituting c_i from equation (6) results in the more convenient expression:

$$p_i = p_e \frac{m_i \delta_i}{\sum_{k=1}^{n} m_k \delta_k} \tag{11}$$

The effective displacement is now defined such that the work done by the SDOF force is equivalent to the work done by the MDOF force system, i.e.:

$$p_e \delta_e = \sum_{i=1}^{n} p_i \delta_i \tag{12}$$

Solving (12) for δ_e and substituting for p_i from equation (11) yields the expression for the displacement of the equivalent SDOF structure:

$$\delta_e = \frac{\sum_{i=1}^{n} m_i \delta_i^2}{\sum_{i=1}^{n} m_i \delta_i} \tag{13}$$

The stiffness of the equivalent SDOF structure is simply

$$K_e = \frac{p_e}{\delta_e} \tag{14}$$

In order to use response spectra for design, the effective damping of the equivalent SDOF structure must also be defined. This may be approximated by first relating the expected damping in each member to the local displacement ductility demands, and then combining the results in a smeared damping factor for the structure. A number of authors have proposed relationships between hysteretic damping and ductility [5], with the form of the expression depending on the hysteretic model. For example, Shibata and Sozen [7] proposed

$$\xi_i = 0.2\left\{1 - \left[\frac{1}{(\mu_{\delta i})^{1/2}}\right]\right\} + 0.02 \qquad \text{i=1,2,...,m (number of members)} \tag{15}$$

where it should be noted that the indices now refer to members rather than degrees-of-freedom. This expression includes a constant equal to 0.02 to represent the viscous damping. The smeared damping factor may be evaluated using a technique such as the one suggested by Shibata and Sozen [7].

$$\xi_e = \sum_{i=1}^{m} \left(\frac{Q_i}{\sum_{k=1}^{m} Q_k} \right) \xi_i \tag{16}$$

where

$$Q_i = \frac{L}{6(EI)_i}\left(M_{ai}^2 + M_{bi}^2 - M_{ai}M_{bi}\right) \tag{17}$$

Note that this method requires an initial structural analysis to determine the expected member end moments.

4. THE DISPLACEMENT-BASED DESIGN PROCEDURE

The displacement-based design procedure is outlined below, with the steps summarised in the flow chart of Figure 6.

Displaced Shape

The first step is to define an initial displaced shape for the structure. To achieve uniform damage levels throughout the structure, the desired displaced shape may be reasonably based on the local drift limits for the piers.

$$\delta_{di} = drift * h_i \tag{18}$$

The notation δ_d is adopted to indicate the "desired displacement" which is imposed on the structure.

Damping

Using the desired displacement limit for each pier and the current member properties, the member ductility demands are defined, and hence the hysteretic damping of each member according to a relation such as the one given in equation (15). Damping properties of the structure play an important role in displacement based design. The stiffness (and strength) demand for the structure is largely a function of the damping, which is in turn a function of the member ductility. Explicit consideration of the damping coefficient in each member thus allows the designer to take into account many aspects of the expected hysteretic response of members rather than simply the ductility. Note, however, that there are no *specified* ductility demands; the values are calculated only as a convenience in the calculation of damping properties.

The Equivalent SDOF Structure

The displaced shape and member damping values are used to determine the displacement and damping of the equivalent SDOF structure according to equations (13), and (16). The displacement response spectra is then entered to determine the period of vibration of the equivalent SDOF structure, T_e. From the period, the effective stiffness and force in the equivalent SDOF structure can be calculated.

$$K_e = \frac{4\pi^2 m_e}{T_e^2} \tag{19}$$

$$p_e = K_e \delta_{de} \tag{20}$$

The effective force on the equivalent SDOF structure is then used to determine the lateral force distribution on the MDOF structure in accordance with equation (11).

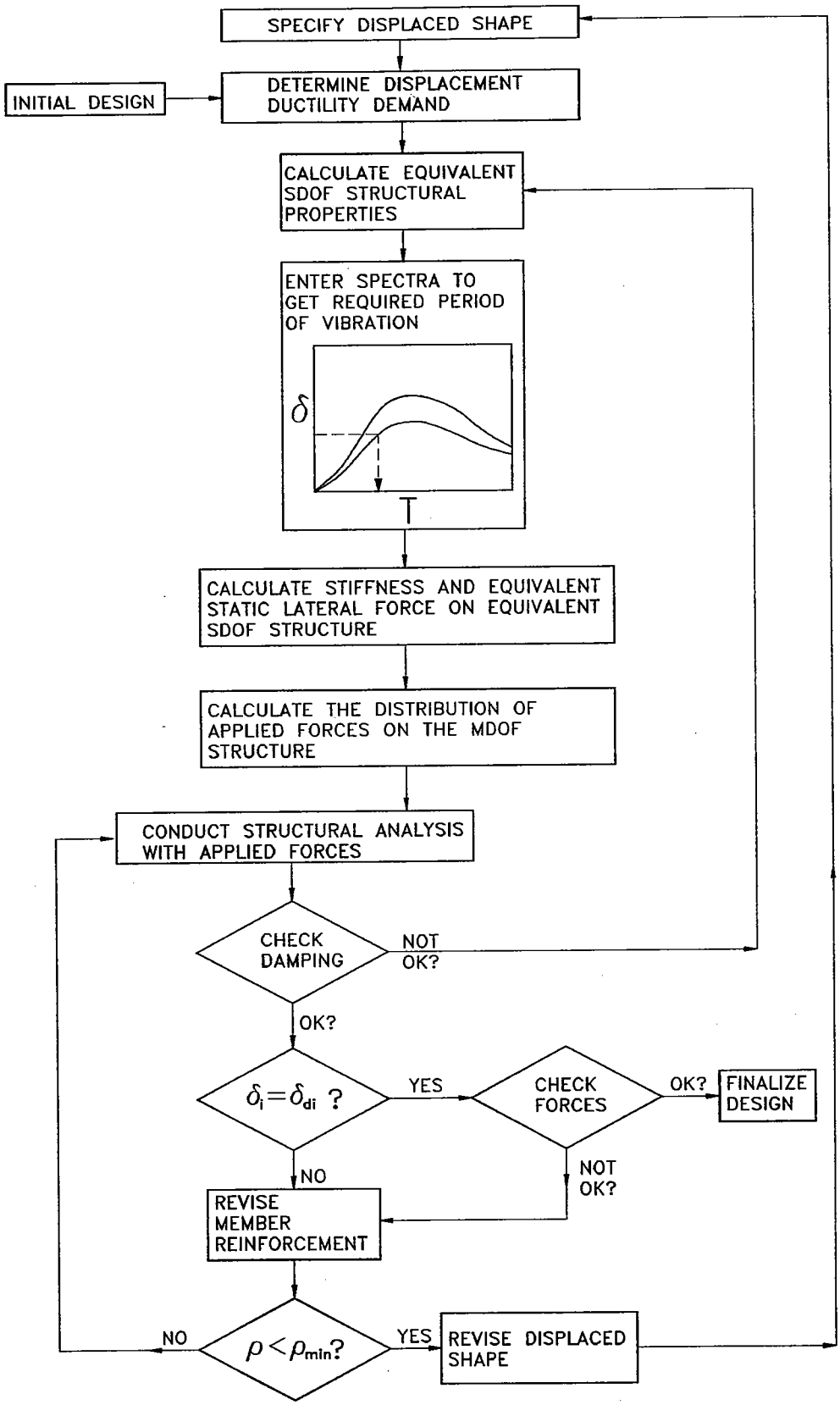

Figure 6 Flow Chart for Displacement-based Design of MDOF Bridge Structures

Structural Analysis

The next step is to perform a structural analysis to determine the member forces and displacements under the applied force distribution. The displacement based design process requires explicit consideration of the strongly nonlinear response of RC structures in the structural analysis phase of the design. For this, a nonlinear "pushover" analysis under monotonically increasing loads would be the ideal tool. It is possible, and perhaps preferable in the initial stages of design, to make use of simple elastic analysis tools provided that the decreased stiffness characteristics of members displaced beyond the elastic limit are appropriately considered. The substitute structure method [7] is well suited to this process.

The fundamental criteria to be satisfied in the displacement based design is that the calculated structural displacements from the linear analysis are equal to the desired displacements, within a specified tolerance.

$$\delta_i \stackrel{?}{=} \delta_{di} \pm tol \tag{21}$$

Design Iterations

If the calculated displacements do not match the desired displacement distribution, then the stiffness of the piers must be appropriately modified by changing the reinforcement or the pier geometry. Once the desired displaced shape is achieved, the forces in the members must be checked against the member strength. The process is continued until the displaced shape matches the desired one, with sufficient capacity in all members to resist the applied force distribution.

It will often happen in bridge structures that the reinforcement required to achieve the desired stiffness is less than the minimum reinforcement requirements specified by the code. In this case, it is not possible to achieve the desired displaced shape, so the displaced shape must be revised accordingly. The new displacement may simply be assumed to be directly proportional to the ratio of the required reinforcement to the minimum reinforcement:

$$\begin{aligned} \rho_{min} \le \rho_{req'd} \qquad & \delta_d^{(new)} = \delta_d^{(last)} \\ \rho_{min} > \rho_{req'd} \qquad & \delta_d^{(new)} = \left(\frac{\rho_{reqd}}{\rho_{min}}\right)\delta_d^{(last)} \ge \delta_{d\,\min} \end{aligned} \tag{22}$$

With a new displaced shape, the entire process must be started anew.

5. EXAMPLE BRIDGE DESIGN

The proposed design procedure was evaluated by applying it to the two bridges shown in Figure 7. Each had four 50 meter spans, with three columns of different heights. In the simplified linear structural analysis model, the bridge deck was assumed to be pinned at the abutments, and the piers were assumed to be fully fixed at the base and pinned at the connection to the bridge deck. The first bridge was symmetrical, with pier heights approximately in proportion to the expected displaced shape of the unconstrained bridge deck (2-3-2). The second bridge was strongly asymmetrical, with pier heights in the proportion 2-1-3. The design of both bridges using force based criteria is presented in reference [5].

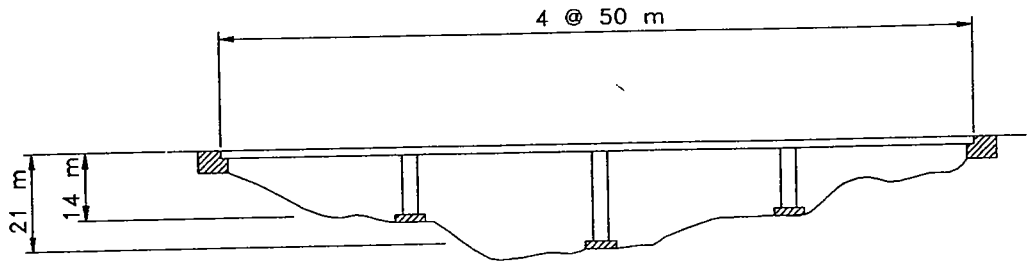

SYMMETRICAL BRIDGE 232

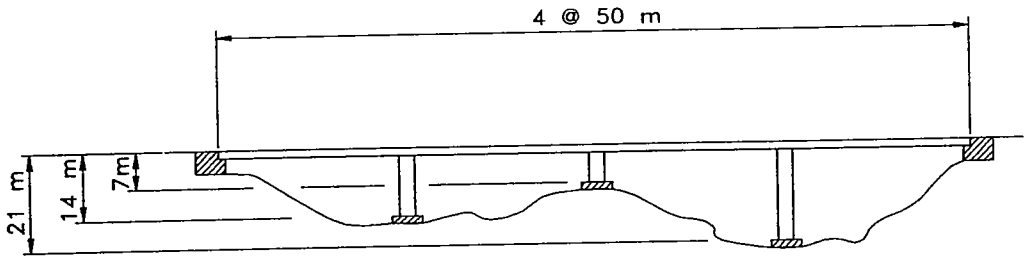

ASYMMETRICAL BRIDGE 213

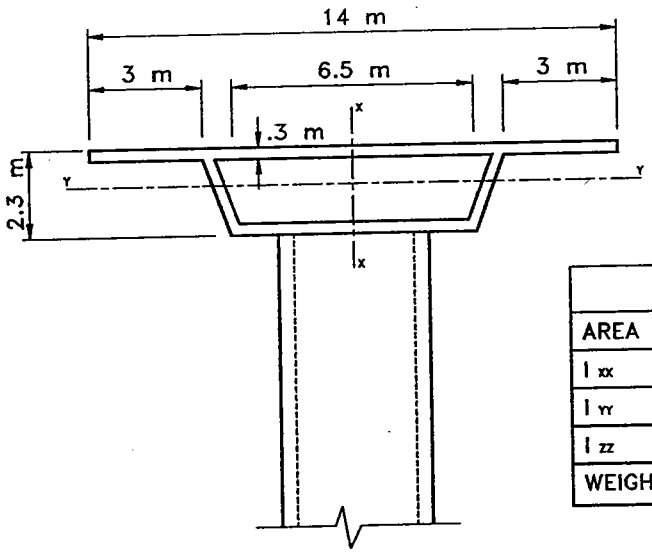

SECTION PROPERTIES

		DECK	PIER
AREA	m^2	6.88	4.16
I_{xx}	m^4	87.24	7.39
I_{yy}	m^4	5.26	0.67
I_{zz}	m^4	12.7	
WEIGHT	kN/m	200	104

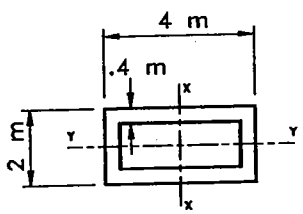

Figure 7 **Elevations and Section Properties of Symmetrical and Asymmetrical Bridges Used to Evaluate the Design Procedure**

Symmetrical Bridge Design

In the design of the symmetrical bridge, the initial target displaced shape was determined by specifying a desired drift of 1% in each of the piers, or displacements of .14m, .21m, and .14m respectively at the top the piers (see Table 1). Using the lumped masses and displaced shape specified in Table 1, the equivalent SDOF structure was defined as described in Section 3, resulting in a desired displacement of 0.17m. Entering the displacement spectrum defined in Section 2 with an assumed damping of 0.06 yielded a target period of vibration of 1.40 seconds, and the calculated force distribution shown in Table 1.

As an initial design approximation, all piers were assumed to have minimum reinforcement (0.5%). Properties of the substitute structure were determined by assuming that each pier acted as a simple cantilever with a linear distribution of curvature up to yield, and constant curvature in the plastic hinge zone at the column base. The assumed plastic hinge length was given by [2]

$$l_p = 0.08h + 0.022 d_b f_y \tag{23}$$

Linear analysis of the substitute structure resulted in displacements of .142m, .205m, and .142m respectively in the piers, and a calculated period of 1.39 seconds. Calculated moments were nearly equal to the pier moment capacities. In other words, the initial assumed design immediately satisfied the design criteria. However, evaluation of the damping according to equations (15)-(17) revealed that the initial assumption of the damping was incorrect, and that a damping value of 0.052 would be more appropriate. With the improved damping estimate, the target period for the structure became 1.32 seconds, and the subsequent increased design forces were those shown in Table 1. Under the new force distribution, two iterations on the pier reinforcement were necessary to satisfy the design requirements.

Several aspects of the design process are illustrated in Figures 8-10. In Figure 8, the target displaced shape is shown as three discreet points, and the calculated displaced shapes from four successive design iterations are shown as lines. The first calculated displaced shape (iteration 1) was quite satisfactory, but with the updated damping and force distribution, the displacements of the same structure (iteration 2) exceeded the desired displacements at all degrees of freedom. Successive increases in the pier reinforcement (iterations 3 and 4) stiffened the structure, and reduced the displacements to near the target level. Figure 9 illustrates the convergence of the structure first mode period to the targets for the equivalent SDOF structure. Finally, Figure 10 illustrates the error in the displacement and force distributions for each iteration. The displacement error was calculated at each step by subtracting the calculated values from the target values, and dividing the RSS of the error by the RSS of the target displacements. Similarly, the error in moments was calculated as the difference between the calculated moment and the pier moment capacity. For the symmetrical bridge, the errors in displacements and moments were very similar.

Table 1 Design of the Symmetrical Bridge

Pier	Lumped Mass (kNs^2/m)	Desired Displacement (m)	First Force Distribution (kN)	Second Force Distribution (kN)	Geometrical Reinforcement Ratio	Displacement Ductility Demand	Calculated Maximum Displacement ADAPT IC
1	1056	0.140	2997	3330	0.75 %	2.2	0.140
2	1074	0.210	4572	5081	0.60 %	1.5	0.207
3	1056	0.140	2997	3330	0.75 %	2.2	0.140

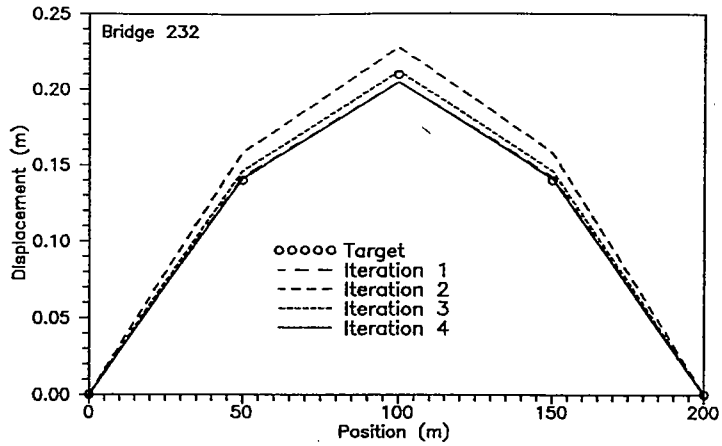

Figure 8 Convergence of the Displaced Shape for the Symmetrical Bridge Design

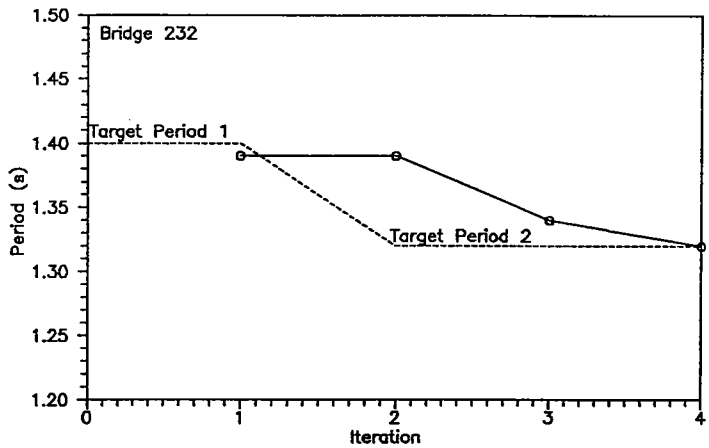

Figure 9 Convergence of the Period of Vibration for the Symmetrical Bridge Design

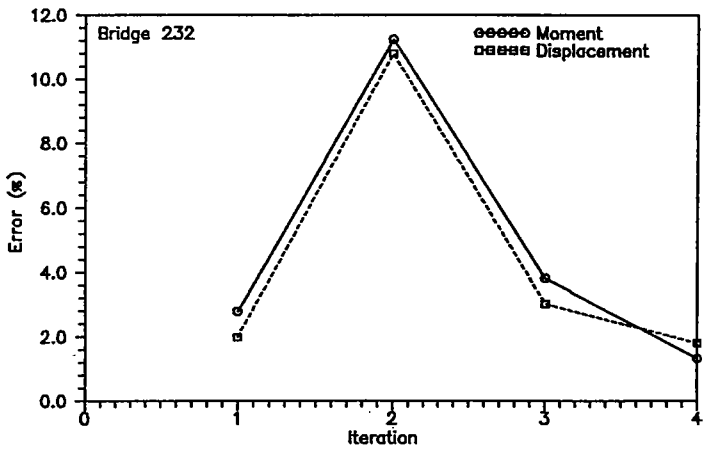

Figure 10 Convergence of Displacement and Moment Capacity Errors for the Symmetrical Bridge Design

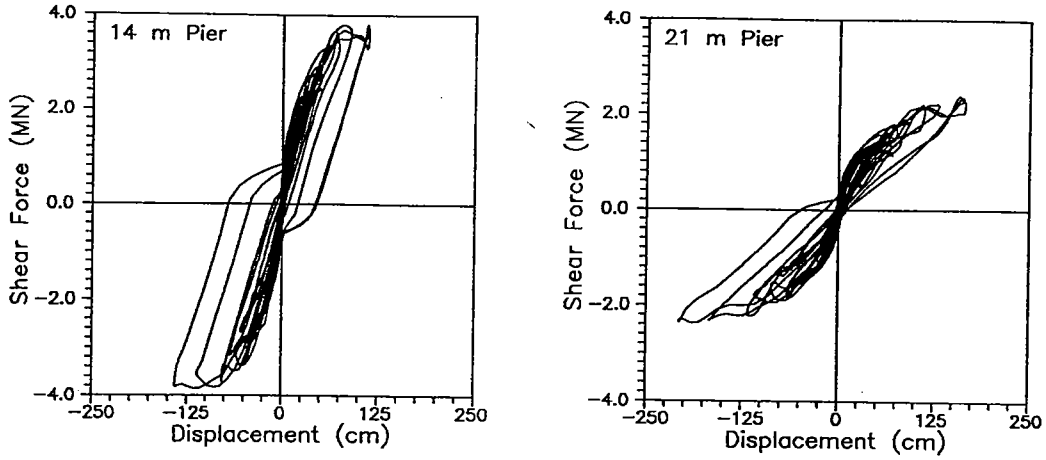

(a) (b)

Figure 11 Shear vs Dispalcement Response of (a) an Exterior Pier, and (b) the Interior Pier from the Nonlinear Analysis of the Symmetrical Bridge

Following the design, a nonlinear analysis of the bridge was conducted using the computer code ADAPT-IC [3], subjecting the bridge to an artificially generated record developed to match the EC8 spectra. Similar analyses were presented in [6] for bridges designed using force-based methods. Hysteretic response of the individual bridge piers is shown in Figure 11. As shown in Table 1, the calculated maximum displacements from the nonlinear analysis agree very well with the desired design displacements. While such close agreement may not be expected from analysis with more realistic ground motion acceleration records, the results indicate that the basis of the design procedure is sound.

Asymmetrical Bridge Design

The asymmetrical bridge chosen to evaluate the design process poses several problems to the designer. As discussed by Calvi et al. [1], the relationship between the displaced shapes of the piers alone and of the bridge deck alone gives an indication of the irregularity of the bridge. When the displaced shape of the piers and the deck coincide, as in the symmetrical bridge discussed above, the dominant vibration mode is close to the mode assumed in the design, and the design forces and ductility demands in the piers can be reasonably well predicted. However, nonlinear time-history analyses of very irregular bridges tend to indicate ductility demands in the piers much greater than the behavior factor used in the design. Because of the difficulty of achieving uniform damage levels in the piers of such irregular bridges, the asymmetrical bridge discussed below was considered to provide an extreme challenge to the design process.

The initial assumed shape was based on uniform pier damage at a drift level of 0.6%. Because the natural mode shape of the bridge deck alone was significantly different than that desired for the piers, the deck was expected to constrain the two exterior piers, thus reducing the displacement and force demands to very low levels, and reducing required reinforcement to less than the minimum reinforcement level (0.5%). Conversely, the bridge deck would drive the center pier to displacements greater than the desired design displacements. Following the

procedure outlined in Figure 6, it was expected that the design process would, after several iterations, result in a new displaced shape which reflected the interaction of the piers and the deck.

The actual progression of the target and calculated displaced shapes is shown for a few selected iterations in Figure 12. The initial structural design assumed minimum reinforcement in all piers. At iteration 2, the calculated displaced shape indicated, as expected, that the target displacement was exceeded in the central pier, and not achieved in the exterior piers. Because the exterior piers were already at minimum reinforcement, the displaced shape was revised according to equation (22), with the result shown as target 2 in Figure 12. Because the applied forces were proportional to the displaced shape, the new shape resulted in decreased applied forces in the exterior piers, and increased force in the interior pier. Furthermore, the decrease in the desired displacements in the exterior piers decreased the effective displacement of the equivalent SDOF structure, thus reducing the target period of vibration, and increasing the total applied force on the structure. With the increase in total force, the displacements in all piers exceeded the targets in the next step (iteration 3), and the moment demand on the center pier increased dramatically. Increasing the reinforcement in the central pier improved the displaced shape, but, as shown in Figure 14, several iterations were required to stabilise the error in the moments, and after nine iterations, the error in the moments was still greater than 20%. The end result was a continuous cycle of increasing strength demand in the interior pier, until the majority of the seismic force was resisted by the short center pier -- the pier with the least capacity for ductile inelastic displacement.

The failure of the design process resulted from the attempted imposition of a single dominant mode shape on a structure whose natural modes of vibration were all significantly different from the chosen mode. Figure 15 shows the calculated mode shapes, periods, and participating mass for the three vibration modes of the bridge, assuming initial elastic stiffness of all piers with minimum reinforcement. Note that the first two modes have quite similar periods with large participating masses in both modes; no single mode can therefore be considered to be clearly dominant. For comparison, mode shapes and periods of the symmetrical bridge are given in Figure 16. In this case, with 96.1% participating mass in the first mode and 0% in the second mode, the first mode completely dominated the behavior of the bridge, and the reduction of the MDOF structure to an SDOF structure with a constant displaced shape was well justified.

Nonlinear analysis of the asymmetrical bridge, with pier reinforcing rations of 0.5%, 0.92%, and 0.5% for the 14 m, 7 m, and 21 m piers respectively [5], confirmed that the displaced shape for such bridges may be extremely erratic, with no single shape dominating the response. The equivalent SDOF displacement defined in Section 3 can serve as a measure of the irregularity of the response, if it is calculated for the predicted displaced shape at each time step of the nonlinear analysis. Figure 17 shows the calculated equivalent SDOF displacement, normalised to the displacement of the interior pier, from analyses of both the symmetrical and asymmetrical bridges, also showing the values assumed in the first design steps, and values corresponding to the first and second modes shown in Figure 15. From Figure 17 it is clear that the assumed displaced shape for the symmetrical bridge was in close agreement with the nearly constant shape from the nonlinear analysis. On the other hand, no consistent shape emerged from the analysis of the asymmetrical bridge.

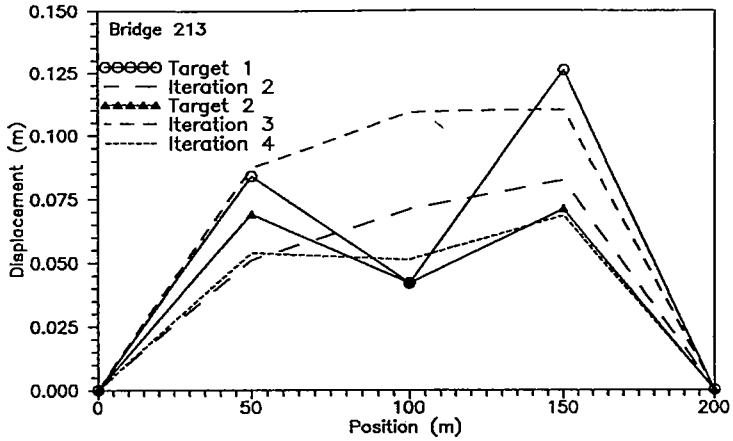

Figure 12 Convergence of the Displaced Shape for the Asymmetrical Bridge Design

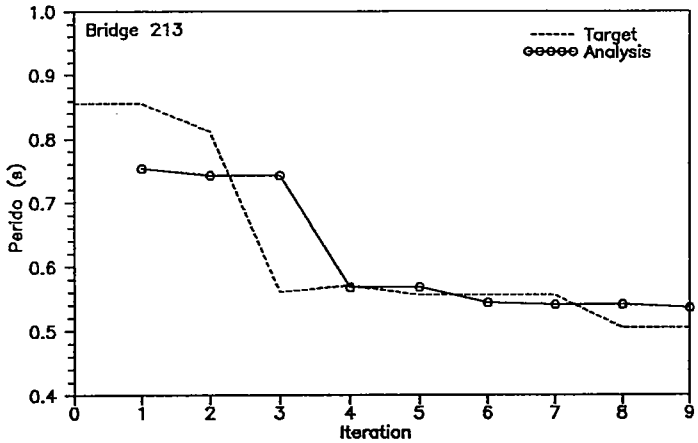

Figure 13 Convergence of the Period of Vibration for the Asymmetrical Bridge Design

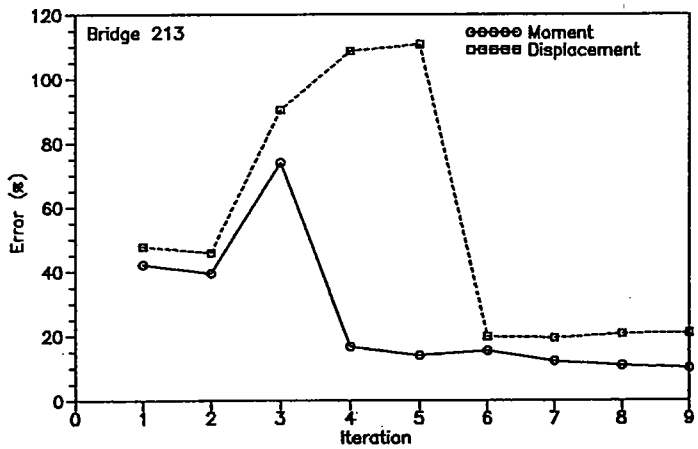

Figure 14 Convergence of Displacement and Moment Capacity Errors for the Asymmetrical Bridge Design

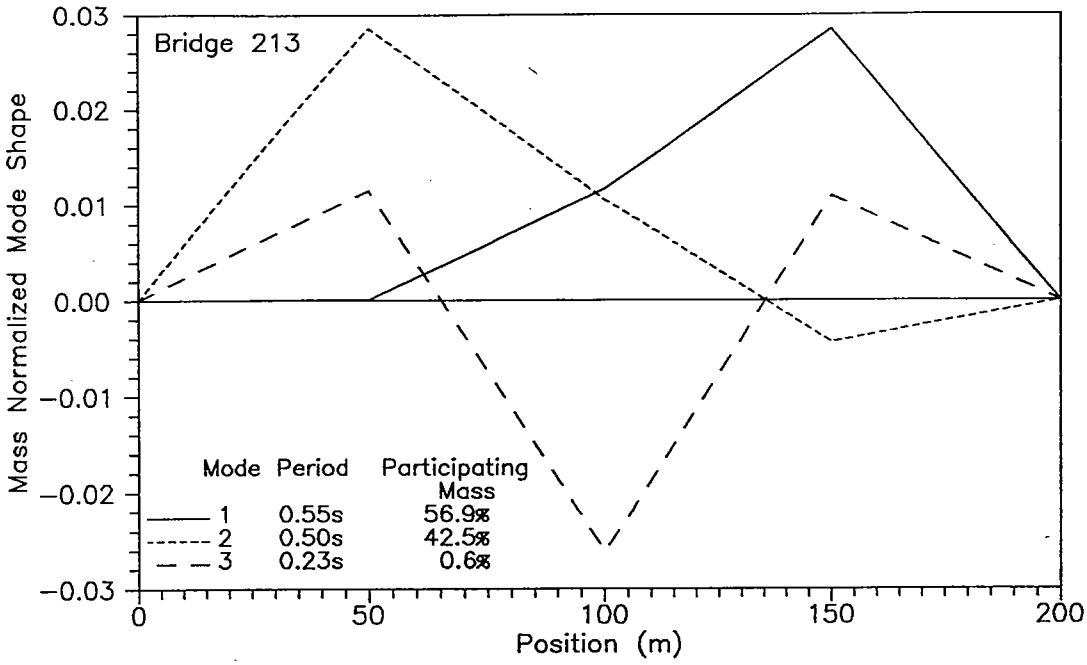

Figure 15 Mode Shapes and Associated Periods of Vibration for the Asymmetrical Bridge (213) Assuming the Initial Elastic Stiffness for All Piers with Minimum Reinforcement

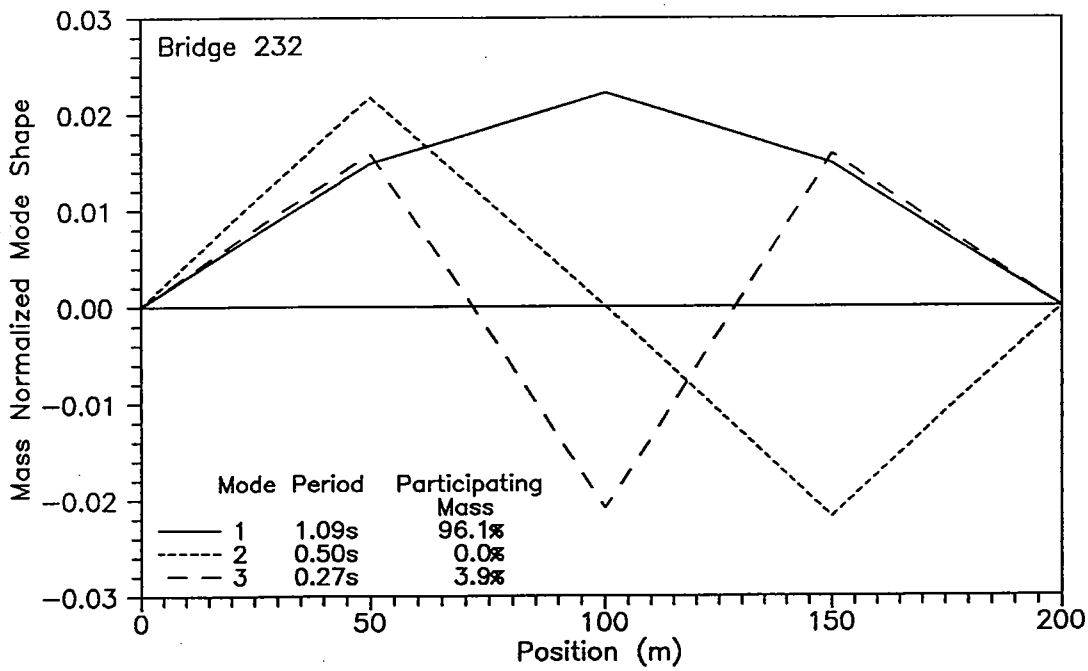

Figure 16 Mode Shapes and Associated Periods of Vibration for the Symmetrical Bridge (232) Assuming the Initial Elastic Stiffness for All Piers with Minimum Reinforcement

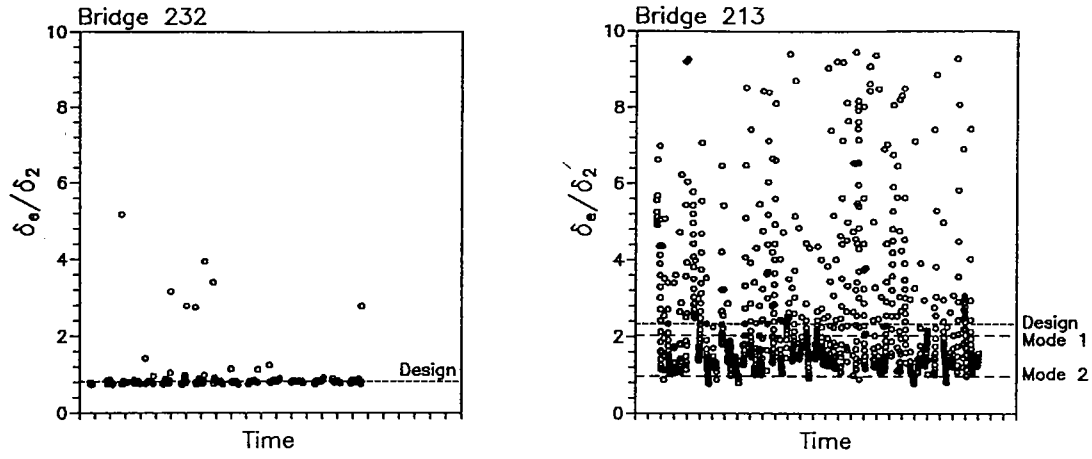

(a) (b)

Figure 17 Calculated Equivalent SDOF Displacement from the Nonlinear Analysis of (a) the Symmetrical Bridge, and (b) the Asymmetrical Bridge

The exercise with the asymmetrical bridge showed that irregular structures require an explicit consideration of several modes of vibration, and that the assumption of a single dominant mode shape is unwarranted. The next logical step will be to extend the displacement based design method to the consideration of multiple modes, and to compare the effectiveness of such an approach to the analogous force-based modal analysis.

6. CONCLUSIONS

A displacement-based seismic design procedure for MDOF structures has been presented, with example designs of regular and irregular bridges. The process, analogous to an equivalent static lateral load procedure, is based on the assumption of a displaced shape for the structure, and the subsequent reduction of the system to an equivalent SDOF system. With the determination of a desired displacement and damping in the equivalent SDOF structure, displacement response spectra are used to determine the required stiffness of the structure, and hence the applied force. Assuming that the applied forces in the MDOF structure are distributed in proportion to the displacements, the structure is analysed under the calculated force distribution, and the member reinforcement designed accordingly. The process is repeated until the stiffness and displaced shape of the structure converge to those specified in the design, with sufficient moment and displacement capacity in each member to satisfy the demand. The process was shown to work well for the design of a simple symmetrical bridge.

The displacement-based design process offers several advantages over a force based process, among them the ability to explicitly consider the displacement demand (i.e. damage) in each member rather than assigning a single, force-based global behavior factor to the structure. The required force to be resisted becomes largely a function of the damping, and thus is related directly to the energy dissipation, hysteretic characteristics, and the acceptable damage on a local level.

Consideration of the complete design process and its application to two bridge examples also highlighted potential shortcomings of the method. Examination of simplified displacement

response spectra showed that for structures large displacements the required period of vibration becomes indeterminate, since the displacement is constant over a range of periods. A careful review of displacement response spectra to determine appropriate smoothed spectra for design would be required before displacement-based design could be considered for any general class of structures. Secondly, the displacement-based method proposed shares with the force-based equivalent static lateral load method the inability to handle structures with several prominent modes of response rather than a single dominant mode, particularly when minimum reinforcement requirements restrict the ability of the designer to adjust member properties to the specific needs of the seismic design. Such problems are not insurmountable, but point to the need for more sophisticated analyses for highly irregular bridge structures.

7. ACKNOWLEDGEMENTS

The authors would like to thank Alberto Pavese for his contributions to discussions of this work, and Paolo Moncecchi for his help in conducting the analyses of the bridges.

8. REFERENCES

1. Calvi, G.M., Elnashai, S.A., and Pavese, A., "Influence of Regularity on the Response of RC Bridges", Proceedings of the Second International Workshop on Seismic Design and Retrofitting of Reinforced Concrete Bridges, Queenstown, New Zealand, August, 1994.

2. Eurocode 8: Earthquake Resistant Design of Structures, *Part 1-1: General Rules and Rules for Buildings- Seismic Actions and General Requirements for Structures* and *Part 2: Bridges*, Draft, April 1993.

3. Izzuddin, B.A., and S.A. Elnashai, "ADAPTIC, A program for Adaptive Large Displacement Elastoplastic Dynamic Analysis of Steel, Concrete, and Composite Frames," Report No. ESEE 7/89, Engineering Seismology and Earthquake Engineering, Imperial College, London, 1989.

4. Moehle, J.P., "Displacement-Based Design of RC Structures Subjected to Earthquakes," Earthquake Spectra, Vol 8, No. 3, august 1992, pp. 403-428.

5. Calvi, G.M., P. Moncecchi, e A. Pavese, "Progetto e Analisi Sismica di Ponti in CA", Dipartimento di Meccanica Strutturale, Università degli Studi di Pavia, Rapporto Scientifico n. 51, Giugno 1994.

6. Priestley, M.J.N, "Myths and Fallacies in Earthquake Engineering - Conflicts Between Design and Reality", Proceedings of the Tom Paulay Symposium, "Recent Developments in Lateral Force Transfer in Buildings", La Jolla, California, September 20-22, 1993.

7. Shibata, A., and Sozen, M.A., "Substitute-Structure Method for Seismic Design in R/C", ASCE Journal of the Structural Division, Vol. 102, No. ST1, January, 1976.